

Supporting Information for

Dual-potential electrochemiluminescence film constructed from single AIE luminogens for sensitive detection of malachite green

Zihua Li,^{*a} Yusheng Zhou,^a Yuhan Cui^a and Guodong Liang^{*a}

^aPCFM lab, School of Materials Science and Engineering, Sun Yat-Sen University, Guangzhou, 510275, China.

* Corresponding author: Tel: +86-20-84004033; Fax: +86-20-84004033

E-mail address: lizh259@mail2.sysu.edu.cn; lgdong@mail.sysu.edu.cn

1. Supplementary Table and Figures

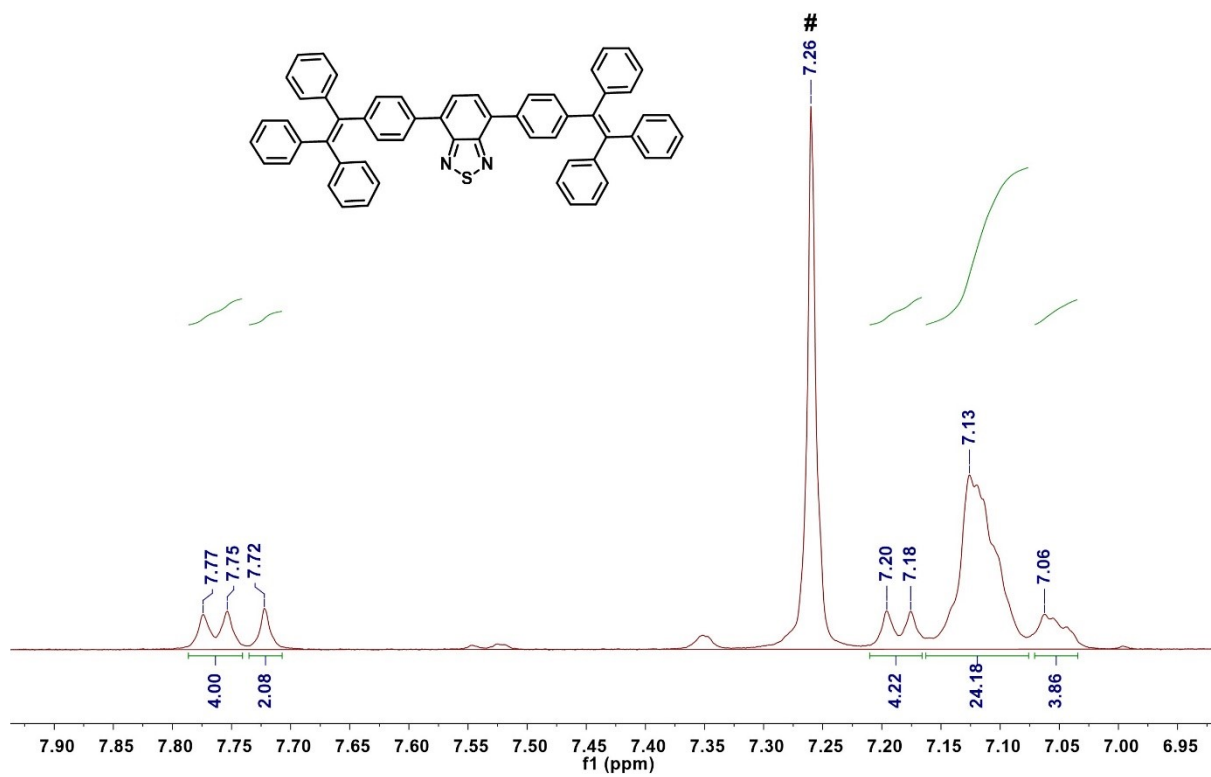


Fig. S1 ¹H NMR spectrum of BTPEBT in CDCl₃ (# CDCl₃).

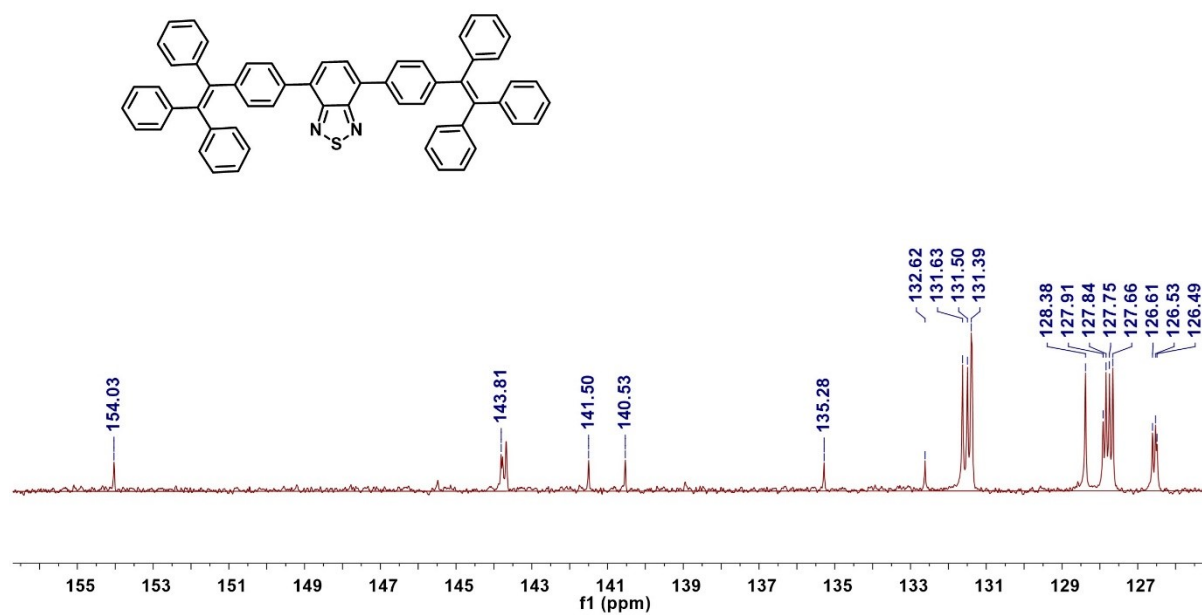


Fig. S2 ^{13}C NMR spectrum of **BTPEBT** in CDCl_3 .

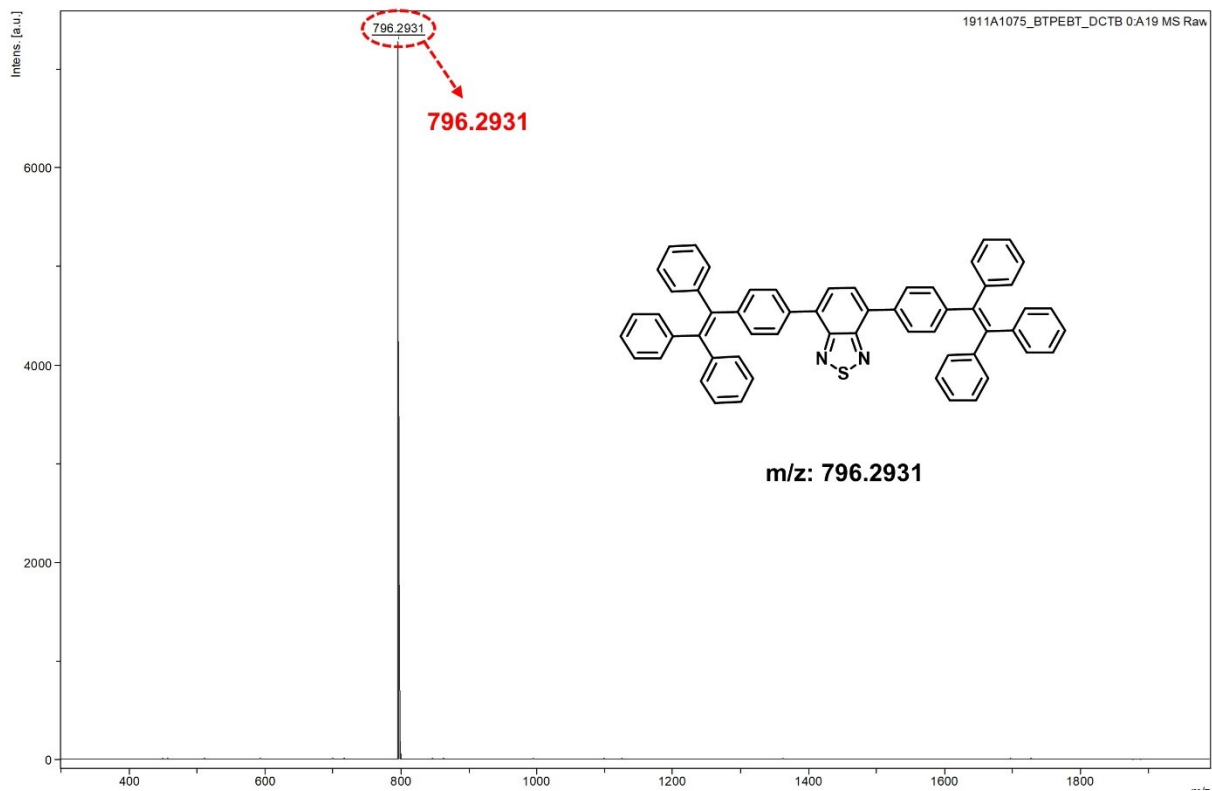


Fig. S3 HRMS spectrum of **BTPEBT**.

Table S1. The absorption and emission wavelength of **BTPEBT** in different solvents.

Compound	λ_{ab} [nm]						λ_{PL} [nm]					
	CH	Tol	DO	THF	DCM	DMF	CH	Tol	DO	THF	DCM	DMF
BTPEBT	418	418	418	418	419	420	513	527	533	541	556	572

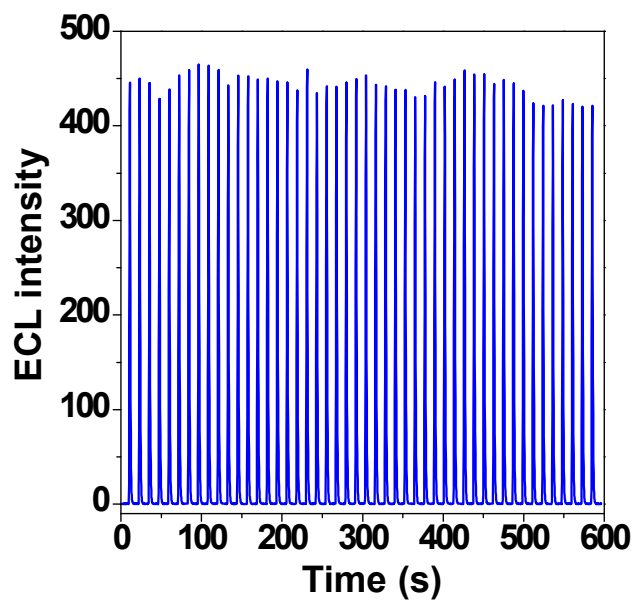


Fig. S4 ECL light transients of **BTPEBT** in DCM solution.

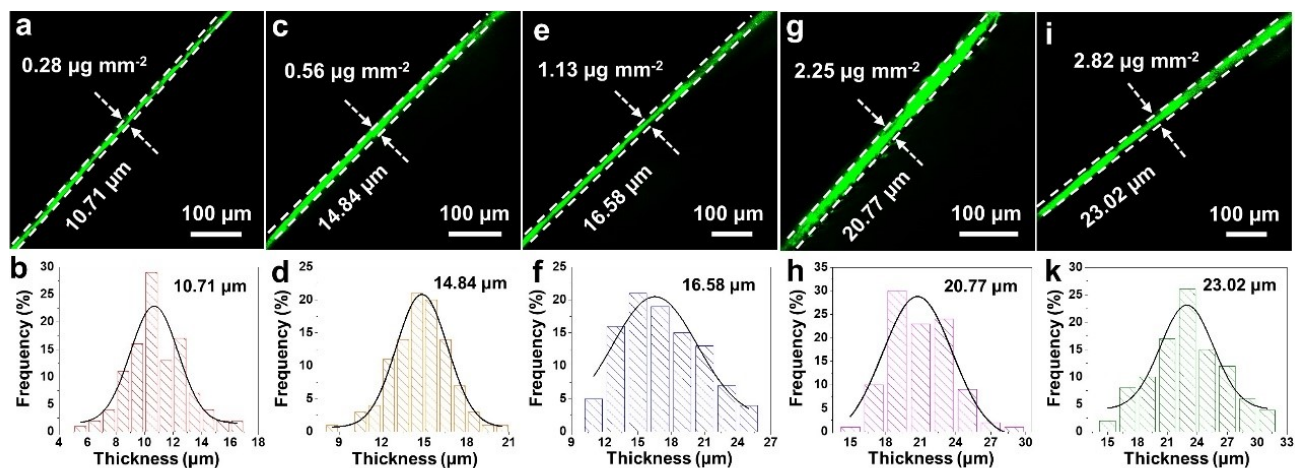


Fig. S5 Fluorescence microscopy images and thickness distribution of **BTPEBT** films on GCE at various loadings of (a) and (b) $0.28 \mu\text{g mm}^{-2}$, (c) and (d) $0.56 \mu\text{g mm}^{-2}$, (e) and (f) $1.13 \mu\text{g mm}^{-2}$, (g) and (h) $2.25 \mu\text{g mm}^{-2}$, and (i) and (k) $2.82 \mu\text{g mm}^{-2}$.

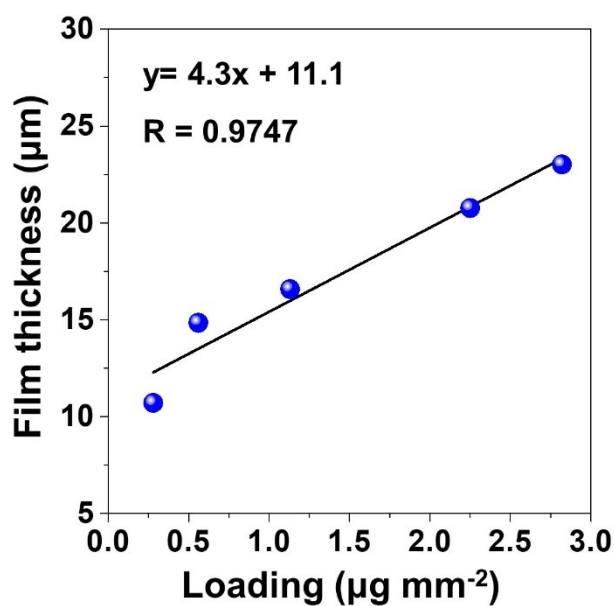


Fig. S6 Plots of thickness of **BTPEBT** film on GCE versus various luminogen loadings.

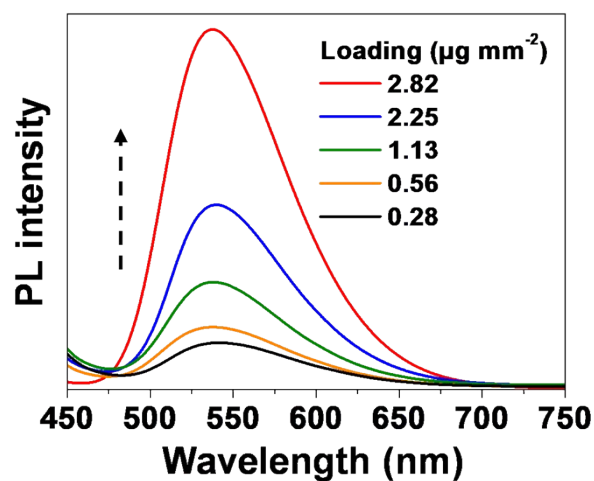


Fig. S7 PL spectra of **BTPEBT** films at various loadings. $\lambda_{\text{ex}} = 400$ nm.

Table S2. Fluorescence quantum yield (Φ_{F}) of solid-state **BTPEBT** films and powder.

BTPEBT	Film					Powder
Loading ($\mu\text{g mm}^{-2}$)	0.28	0.56	1.13	2.25	2.82	
Φ_{F} (%)	46.44	50.18	58.62	58.94	60.71	69.8

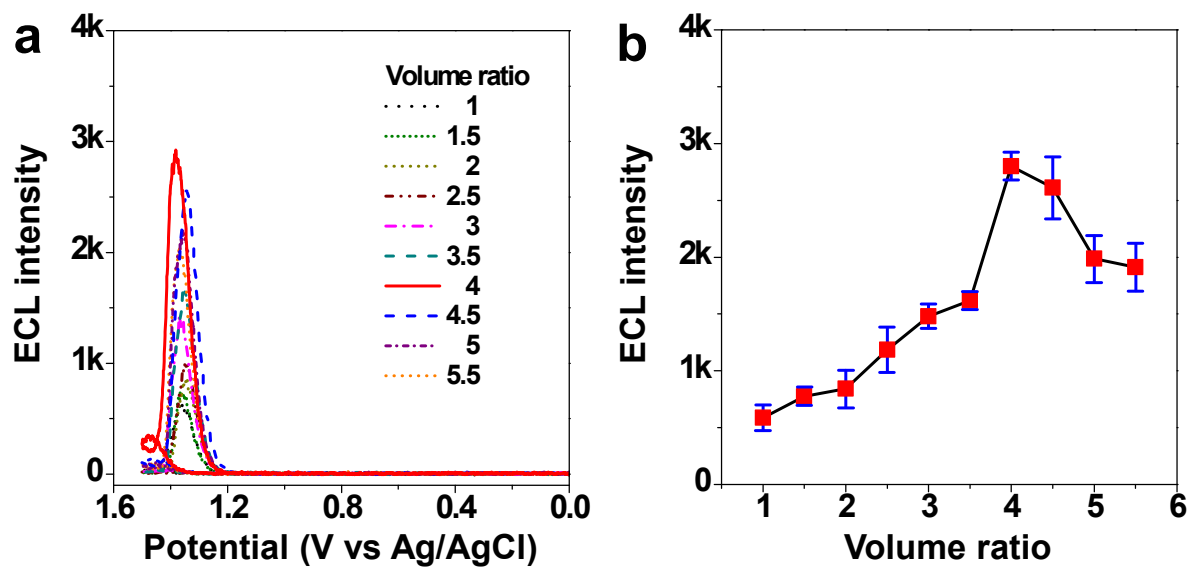


Fig. S8 Optimized ECL intensity of **BTPEBT** films in MeCN/H₂O mixtures containing 20 mM TPrA.

(a) ECL profiles and (b) plots of ECL emission maximum with varied volume ratios of mixtures.

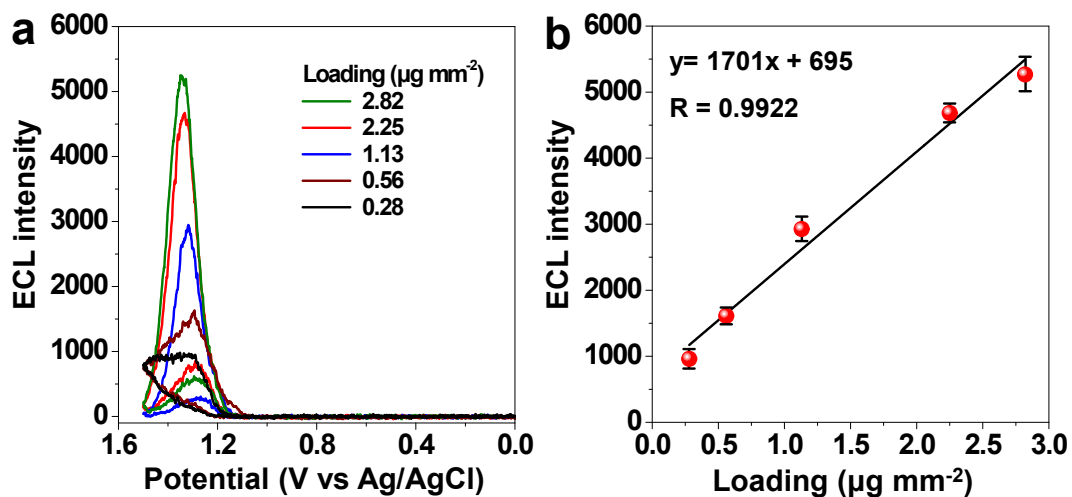


Fig. S9 (a) ECL intensity of the BTPEBT film with different luminogen loadings. (b) Plots of ECL intensity versus different luminogen loadings.

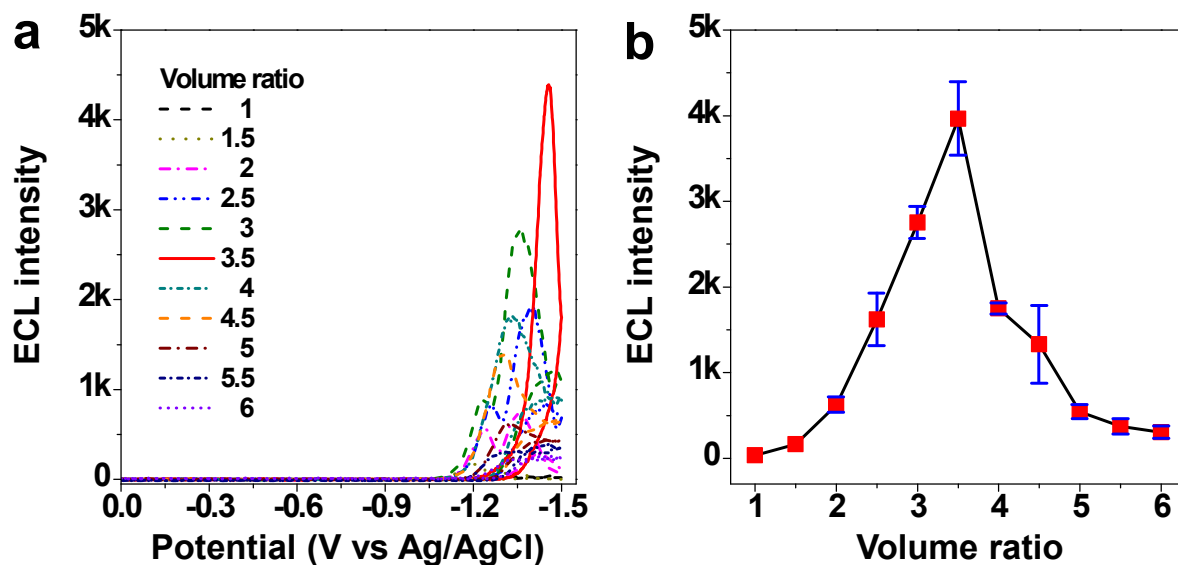


Fig. S10 Optimized ECL intensity of BTPEBT films in MeCN/H₂O mixtures containing 30 mM K₂S₂O₈. (a) ECL profiles and (b) plots of ECL emission maximum with varied volume ratios of mixtures.

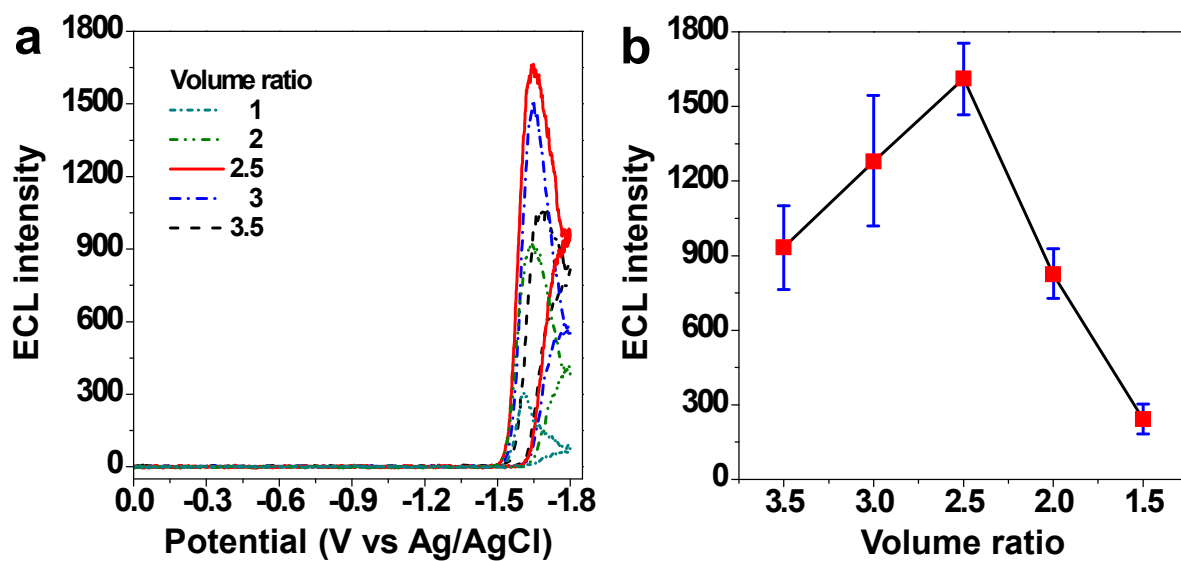


Fig. S11 Optimized ECL intensity of **BTPEBT** films in MeCN/H₂O mixtures containing 32 mM BPO.

(a) ECL profiles and (b) plots of ECL emission maximum with varied volume ratios of mixtures.

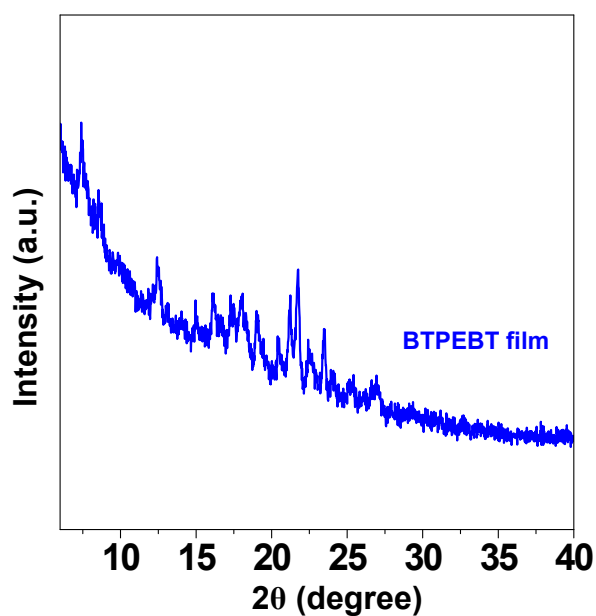


Fig. S12 XRD pattern of the **BTPEBT** film.

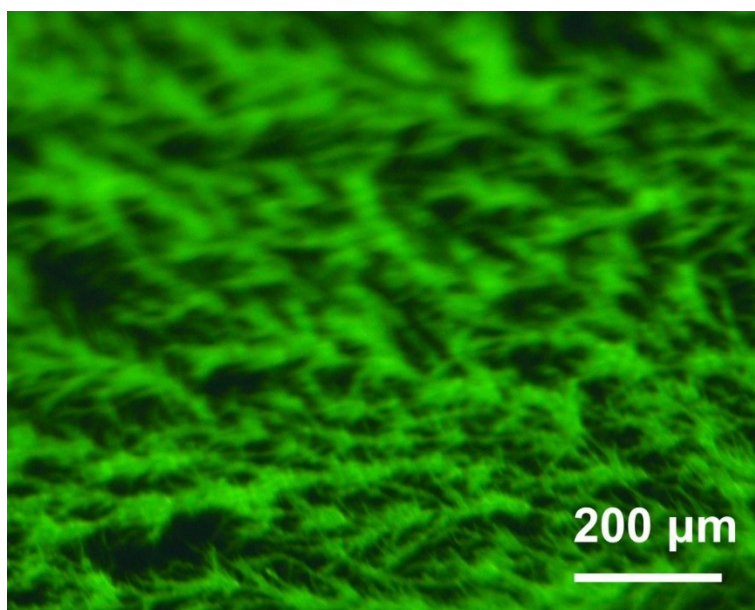


Fig. S13 Fluorescence microscopy image of **BTPEBT** crystals.

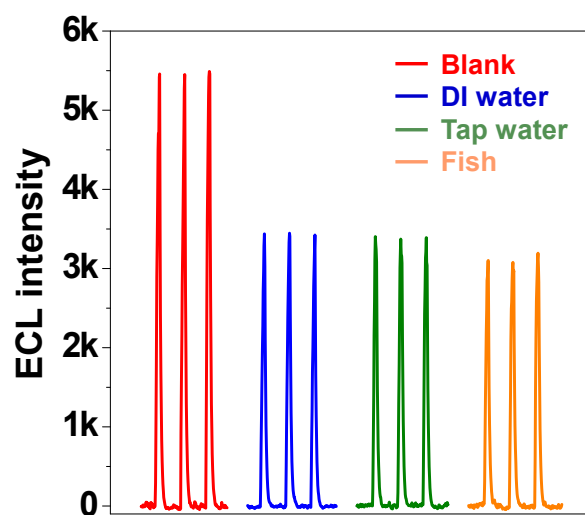


Fig. S14 ECL intensity of the **BTPEBT** film in different MG-spiked samples.

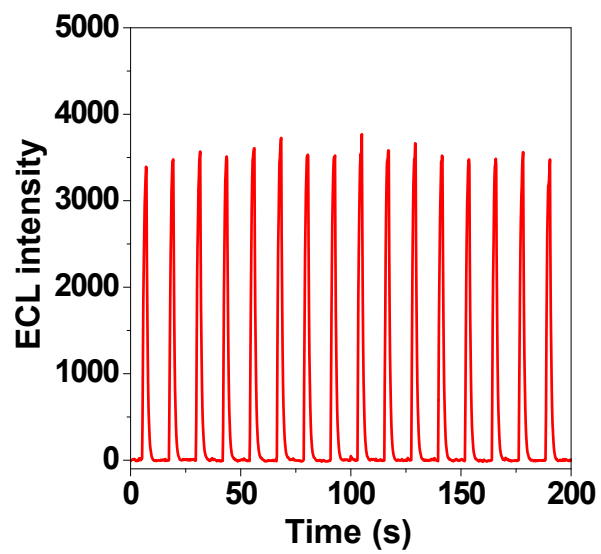


Fig. S15 ECL stability of the recycled **BTPEBT** film with 20 mM TPrA as coreactants.

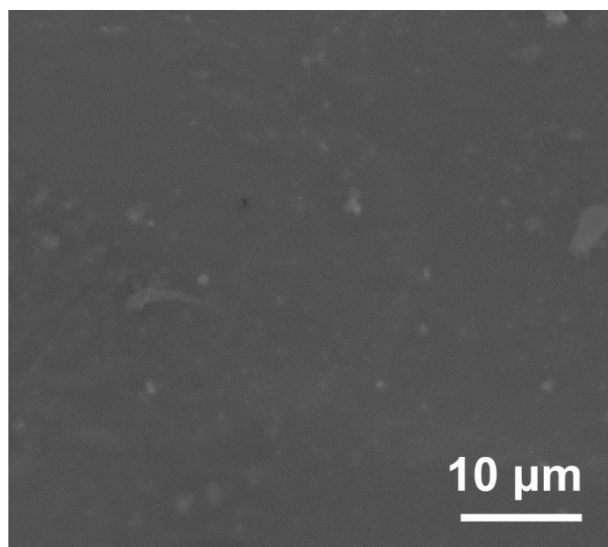


Fig. S16 SEM image of the **BTPEBT** film on GCE after ECL detection.

2. Determination of ECL efficiency

The ECL efficiencies were calculated using the Ru(bpy)₃²⁺/TprA system as reference ($\Phi_{\text{ECL}} = 5.0\%$)

by integration of both ECL intensity and current value versus time for each compound, as described in

Equation (S1)

$$\Phi_x = 100\% \times \left[\frac{\int_a^b ECLdt}{\int_a^b Currentdt} \right]_x / \left[\frac{\int_a^b ECLdt}{\int_a^b Currentdt} \right]_{st} \quad (\text{S1})$$

where x stands for **BTPEBT**, and st represents Ru(bpy)₃²⁺.